THE JOURNAL OF PHYSICAL CHEMISTRY B

Article

pubs.acs.org/JPCB

Solid-State Phase Transitions of DL-Aminobutyric Acid

Carl Henrik Görbitz,*[,†] Fassil Alebachew,[†] and Václav Petříček[‡]

[†]Department of Chemistry, University of Oslo, N-0315 Oslo, Norway

[‡]Institute of Physics, Academy of Sciences of the Czech Republic v.v.i., Na Slovance 2, 182 21, Praha 8, Czech Republic

Supporting Information

ABSTRACT: Four polymorphs are known for the amino acid racemate DL-aminobutyric acid: one tetragonal form *B* and three monoclinic forms *A*, *C*, and *D* for which two solid−solid phase transitions take place between 209 and 337 K. The intermediate form *A*, in space group $P2_1/c$, is known to display disorder in the crystalline state with the ethyl side chain occupying three different conformations. The high temperature form *D* and the low temperature form *C* have been assumed to display a similar type of disorder in the space group $C2/c$. The present investigation, on the basis of high quality crystal structures at 100 K (*C* form), 220 K (*A* form), 295 K (*A* form), and 295 K (*D* form), provides updated results for all three forms and in particular demonstrates that the $A \rightarrow C$ and $A \rightarrow D$ transitions in fact involve only a partial space group conversion, so that two monoclinic phases are simultaneously present at high and low temperatures. To the best of our knowledge, such a phenomenon has not been observed previously for an organic molecule. The nonroutine refinement of the crystallographic data was performed with a specially adapted version of the program JANA2006. The observed polymorphs are compared with those found for DL-norvaline, DL-norleucine, and DL-methionine.

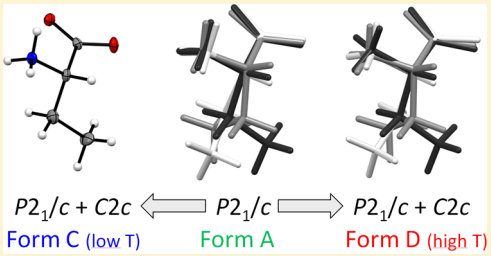

1. INTRODUCTION

In 1951, Dawson and Mathieson observed that the racemates of amino acids with unbranched side chains crystallized in two monoclinic forms,[1] where the one with space group $P2_1/a$ was referred to as α and that with $I2/a$ as β (or $P2_1/c$ and $C2/c$ with different cell settings). Both polymorphs are known for DL-norvaline (DL-Nva) with a *n*-propyl side chain,[2] for DL-norleucine (DL-Nle)[3,4] with a *n*-butyl side chain, and for its analogue DL-methionine (DL-Met)[5,6] where $-C^{\delta}H_2-$ has been replaced by −S−. Above 117 °C, α-DL-Nle is furthermore reversibly transformed into the high-temperature γ form,[7,8] which was recently shown to also be monoclinic $C2/c$.[9] DL-Aminobutyric acid (DL-Abu), with an ethyl side chain, has no less than four polymorphs: an ordered tetragonal form *B*[10,11] and three monoclinic forms *A*,[10,12] *C*,[13] and *D*.[14] The interplay between the various polymorphs is shown in Figure 1, which also gives transition temperatures (invariably subject to some variability depending on crystal specimen, heating/cooling rate, etc.). We retained the original phase indicators of Dawson and Mathieson[1] in our recent investigation of DL-Nva,[2] with the β phase occurring at higher temperature than the α phase (as shown in Figure 1), but we indicated that the former should probably be considered equivalent to the DL-Nle γ phase under the assumption that the as yet uncharacterized phase X is also monoclinic $C2/c$. For DL-Met, no high temperature transition to a $C2/c$ form has been found.

The observed Martensitic phase transformations,[8,16] which occur by cooperative, homogeneous movement of atoms rather than by diffusion and with an orientational relationship between the two forms, are extremely rare for molecular crystals.[8] The nature of these intriguing, displacive structural changes, which in addition to X-ray crystallography have been studied by solid-state NMR methods,[17] Raman spectroscopy,[15] and molecular dynamics simulations,[8] is illustrated in Figure 2 using DL-Nle as an example. While hydrogen-bonding patterns within a molecular double layer are largely unaffected, the polymorphs are distinct at the interfaces at the centers of the hydrophobic bilayers. Conceptually, the β- and γ-forms are obtained from the α form by translation of every second molecular double layer half a unit cell length along the *b* axis, Figure 2 a. At the same time, layers are also shifted to various degrees along the *c* axis, Figure 2 b. There is even a small change in the periodicity along the *a* axis as rearrangement of side chains affects the thickness of hydrophobic regions in the crystal, but this phenomenon is barely visible in Figure 2.

Figure 2 also shows that phase transitions may (α to γ) or may not (α to β) be associated with conformational changes for the side chain. Additional examples of the former include α to β transitions for DL-Nva and DL-Met. For DL-Abu, this picture is blurred by the fact that all monoclinic polymorphs have been found to incorporate side chain disorder. Voogd and Derissen[12] used a model with three terminal methyl positions and concluded: "In modification *A* the populations of the three positions are about 50% *trans*, and the remaining 50% almost evenly distributed over *gauche* I and *gauche* II" with the latter torsion angles corresponding to gauche+ (N1−C2−C3−C4 ≈ 60°) and gauche− for the L-enantiomer. These results were in close agreement with earlier results by Ichikawa and Iitaka,[10]

Received: May 23, 2012
Revised: August 2, 2012
Published: August 6, 2012

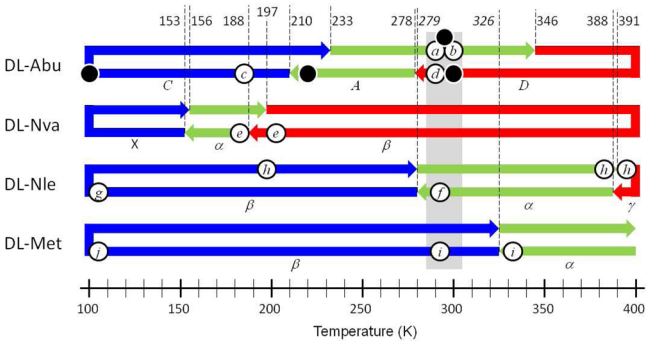

Figure 1. Phase transitions for the racemates of amino acids with linear side chains on cooling (left arrows) and heating (right arrows). Low- and high-temperature phases in space group $C2/c$ (alternative notation $I2/a$) are indicated in blue and red, respectively, and intermediate phases in space group $P2_1/c$ (alternatively $P2_1/a$) are shown in green. See text for details. Phase notations from the literature are given below each racemate; transition temperatures from differential scanning calorimetry (DSC) analysis given on the top are taken from Coles et al.[9] for DL-Nle, from Chatzigeorgiou et al.[15] for DL-Nva, and from this work for DL-Abu (Nakata et al.[14] reported 337 K For the *A* to *D* transition). Hysteresis data are not available for transitions with temperatures in italic type face ($\alpha \rightarrow \beta \rightarrow \alpha$ for DL-Met and DL-Nle). Circles in black indicate single crystal structure determinations carried out here, and white circles represent previous work: *a*, ref 10; *b*, ref 12; *c*, ref 13; *d*, ref 14; *e*, ref 2; *f*, ref 3; *g*, ref 4; *h*, ref 9; *i*, ref 5; *j*, ref 6. The gray box represents room-temperature investigations.

who estimated the trans, gauche+, and gauche− occupancies to 40.0, 36.4, and 23.6%, respectively. For the high-temperature *D* form, Nakata et al.[14] described "statistical disorder of the terminal C_γ atom at the two positions, *T* and *GII*" (trans and gauche−), but did not give detailed estimates for the occupancies. Akimoto and Iitaka,[13] in their refinement of the *C* form, employed a model "in which only the Cγ atom at the *trans* position (*trans* to the amino nitrogen) was taken into account.... The difference Fourier maps of *b* and *a* axis projections indicated that a small proportion of the Cγ atom was still distributed in the *gauche* I (...) and *gauche* II (...) positions. Persistence of the disordered structure even at −90 °C was also reflected by the presence of very diffuse $h + k = 2n + 1$ reflections which should be extinguished on changing to the structure of space group $I2/a$." The associated entry in the Cambridge Structural Database (CSD, version 5.33 of November 2011)[18] with Refcode DLABUT02 is clearly very inaccurate with an *R*-factor of 0.247 and a nonbonded N···O distance of 1.256 Å.

In view of the very interesting properties of the DL-Abu system, which may be compared with recent results for DL-Nva and DL-Nle,[2,9,15,17] the quality of the available crystal structures for the three monoclinic forms, dating back to 1980 and before, was low by modern standards. We here present an updated single crystal X-ray diffraction analysis of *A*-DL-Abu, *C*-DL-Abu, and *D*-DL-Abu.

2. EXPERIMENTAL METHODS

2.1. Materials. The amino acid racemate DL-Abu was purchased from Sigma and was used as received.

2.2. Crystal Growth. About 2 mg of DL-Abu was dissolved in 30 μL of water in a 30 × 6 mm test tube and was sealed with parafilm. A small hole was then pricked in the parafilm, and the tube was placed inside a larger test tube filled with 1 mL of acetonitrile. The system was ultimately capped and was left for three days at 20 °C. Large crystals were formed as the organic solvent diffused into the aqueous solution.

2.3. Differential Scanning Calorimetry (DSC) Measurements. A liquid-nitrogen operated Perkin−Elmer Pyris 1 instrument was used to perform successful heating and cooling DSC cycles of 27.1 mg of dry sample sealed in aluminum pans as the scanning rate was decreased from 40 to 10 K/min. The power and temperature scales of the instrument were calibrated against enthalpy and temperature of *n*-dodecane, *m*-nitrotoluene, *p*-nitrotoluene, and indium standards of >99.7% purity.

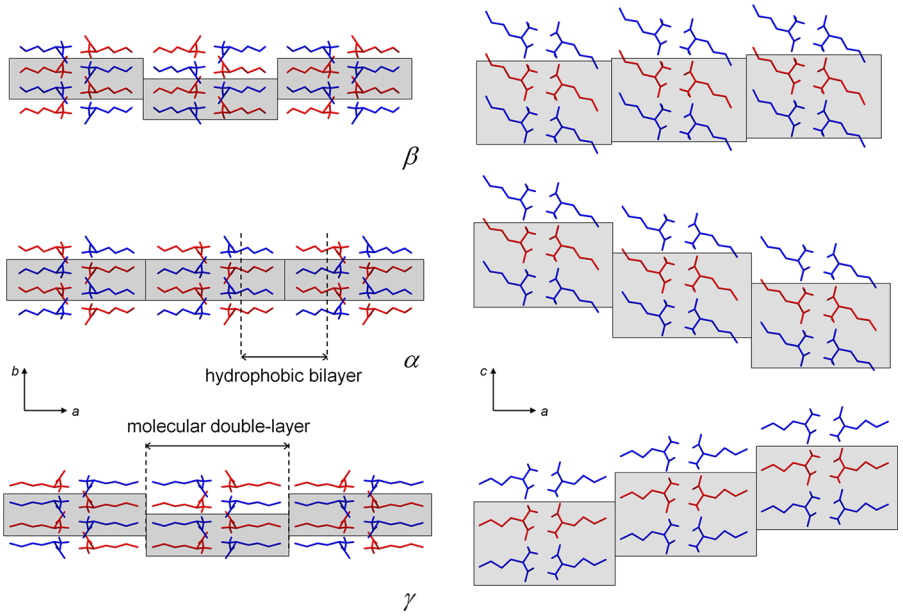

Figure 2. Structural rearrangements upon phase transition for DL-Nle highlighted by gray boxes. L-Enantiomers (S-configuration) are shown in red, D-enantiomers in blue. Views are along the *b*-axis (left column) or the *a*-axis (right column). See text for details. Data have been taken from refs 2, 3, and 9 for the α-, β-, and γ-forms, respectively.

dx.doi.org/10.1021/jp305016k | J. Phys. Chem. B 2012, 116, 10715−10721

The transition temperatures were evaluated by extrapolating the peak high transition temperatures to zero scanning rate.

2.4. Data Collection and Structure Solution. The crystallographic data are reported in Table 1. An initial data collection at 295 K (room temperature, not discussed in detail here) showed that the crystal obtained was of the *A* modification in space group $P2_1/c$. The temperature was then reduced for collection of data at 220 K. The phase transition around 210 K was readily observed by collection of equivalent frames (same sections of the reciprocal lattice) throughout cooling to 100 K for collection of a data set on the *C* form. Finally, the temperature was increased to 360 K and was kept as this level for 1 day to complete the transition to the *D* form for which data were subsequently obtained at room temperature, 295 K. Single crystal X-ray data collections were performed with APEX2[19] with an Apex II single crystal CCD diffractometer and MoK_α radiation (λ = 0.71069 Å). Data integration and cell refinement was performed with SAINT-Plus[20] with subsequent absorption correction by SADABS[21] and structure solution with SHELXTL.[22]

Table 1. Crystal Data

compound	*A*-DL-Abu	*A*-DL-Abu	*C*-DL-Abu	*D*-DL-Abu
chemical formula	$C_4H_9NO_2$	$C_4H_9NO_2$	$C_4H_9NO_2$	$C_4H_9NO_2$
formula weight	103.12	103.12	103.12	103.12
crystal system	monoclinic	monoclinic	monoclinic	monoclinic
space groups	$P2_1/c$	$P2_1/c$	$C2/c$, $B2_1/c$[a]	$C2/c$, $B2_1/c$[b]
space group fractions	1.000	1.000	0.455(4), 0.545(4)	0.404(2), 0.596(2)
T/K	295	220	100	295
a/Å	11.9715(12)	11.8782(9)	24.7705(19)	24.165(16)
b/Å	4.8141(5)	4.8004(4)	4.7114(4)	4.812(3)
c/Å	9.8678(9)	9.8598(7)	9.8854(7)	9.889(6)
β/°	101.011(5)	100.911(4)	108.388(3)	102.081(7)
V/Å^3	558.23(7)	552.04(7)	1094.76(15)	1124.5(12)
Z	4	4	8	8
V_M/Å^3[c]	139.56(2)	138.01(2)	136.85(2)	140.56(15)
$N_{measured}$	6636	6566	11 799	2986
N_{unique}	1452	1536	3157	1941
$N_{observed}$ [$F^2 > 2\sigma(F^2)$]	1217	1285	2538	1355
R_{int}	0.0298	0.0266	0.0365	0.0334
R [$F^2 > 2\sigma(F^2)$]	0.0392	0.0363	0.0479	0.0536
$wR(F^2)$	0.1131	0.1053	0.0705	0.1194

[a] $P2_1/c$ unit cell: a = 11.7984(9) Å, β = 95.037(4)°. [b] $P2_1/c$ unit cell: a = 12.059(8) Å, β = 101.560(7)°. [c] Molecular volume = V/Z

2.5. Structure Refinement. Least-squares refinement of *A*-DL-Abu was carried out in a regular manner with SHELXTL[22] on F^2. As expected, side chain disorder was readily apparent, and a model with whole molecule disorder was adopted, Figure 1 c, as used in our refinement of DL-Nva.[2] The covalent geometries of the three independent disorder parts were linked by SHELXTL SAME 0.004 0.006 commands that restrained corresponding covalent bonds (not involving H) to be similar within an effective standard deviation of 0.004 Å and 1−3 distances to be similar within an effective standard deviation of 0.006 Å effectively putting restraints on covalent angles. All heavy atoms were refined anisotropically, but apart from the three atoms C4_*trans*, C4_*gauche*+, and C4_*gauche*−, which are separated by 1.5 Å or more, equivalent atoms belonging to different disorder parts were constrained to have the same set of thermal parameters to avoid unreasonable values as the result of strong correlation.

The crystal structure of *C*-DL-Abu was first refined to an *R*-factor close to 0.04 in space group $C2/c$, but integration had showed that, as observed by Akimoto and Iitaka (see above),[13] the ignored $h + k = 2n + 1$ reflections were, although systematically weak, clearly not absent. In our previous study of DL-Nva,[2] we did not observe such violations. Rather than interpreting this finding as a sign of side chain disorder, we assumed that an explanation could be that the $P2_1/c$ to $C2/c$ transition, involving sliding of every second layer as shown in Figure 2 and Figure 3 a, was in fact not complete and that a certain fraction of the crystal essentially belonged to the $P2_1/c$ space group even below the transition temperature as shown in Figure 3 b. This meant that it was necessary to refine two simultaneous phases, which is not handled by SHELXTL. Thus, subsequent refinement was carried out by the program JANA2006.[23]

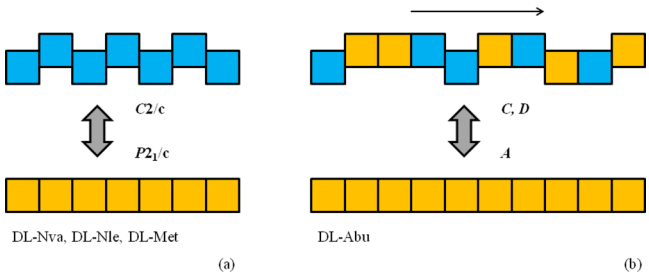

Figure 3. (a) Schematic representation of the systematic sliding of every second layer along the *a*-axis observed for DL-Nva, DL-Nle, and DL-Met. (b) Model showing incomplete sliding of layers for DL-Abu. Moving from left to right, certain molecular double layers of the *C* and *D* forms, colored in blue, have layers to their right that have been translated and thus formally belong to the space group $C2/c$, while other layers, colored in orange, have a nontranslated adjacent layer and thus retain the $P2_1/c$ space group.

The refinement method used by JANA is based on the assumption that coexisting domains $C2/c$ and $P2_1/c$ diffract independently. Then, the observed diffraction intensities are combined from two contributions:

$$I(\mathbf{h}) = vI_1(\mathbf{h}) + (1 - v)I_2(\mathbf{hT})$$

where v is the volume fraction of the component $C2/c$ while I_1 and I_2 are contributions from different domains. The matrix **T**, which transforms indices from the reference indexing system (identical with the standard setting of used $C2/c$) to that for $P2_1/c$ space group, is

$$\begin{bmatrix} 1/2 & 0 & 0 \\ 0 & -1 & 0 \\ 1/2 & 0 & -1 \end{bmatrix}$$

However, in the final stages of the refinement, a nonstandard setting was used for the domain $P2_1/c$ which leads to the space group $B2_1/c$ and to the unit transformation matrix. This allows for easier comparison and restriction of geometrical parameters.

For *C*-DL-Abu, there was no indication of any side chain disorder; the N1−C2−C3−C4 torsion angle is restricted to the trans orientation, and the refinement converged smoothly. Refinement of *D*-DL-Abu followed similar procedures with the

dx.doi.org/10.1021/jp305016k | J. Phys. Chem. B 2012, 116, 10715−10721

added complication that the side chain in this case was disordered over three positions in much the same way as observed initially for *A*-DL-Abu. In the refinement, geometrical restraints equivalent to those used for *A*-DL-Abu were used to overcome problems with strong correlations. Here, the problems are even more pronounced because of the coexistence of two structural phases.

H atoms were always positioned with idealized geometry, and N−H and C−H distances were fixed to 0.91/0.90/0.89 (NH_3), 0.98/0.97/0.96 (CH_3), 0.99/0.98/.97 (CH_2), or 1.00/0.99/0.98 Å (CH), respectively, for the *C*/*A*/*D* form (default SHELXTL values at 100/220/295 K). Free rotation was permitted for amino groups. U_{iso} values were set to $1.2U_{eq}$ (CH and CH_2) or $1.5U_{eq}$ (NH_3 and CH_3) of the carrier atom. Deposition numbers at the Cambridge Crystallographic Data Centre are CCDC 883412 (*A*, 220 K), CCDC 883413 (*A*, 295 K), CCDC 883414 (*C*, $B2_1/c$ phase), CCDC 883415 (*C*, $C2/c$ phase), CCDC 883416 (*D*, $B2_1/c$ phase), and CCDC 883417 (*D*, $C2/c$ phase).

2.6. Molecular Configuration. The crystal structures of amino acid racemates by default contain molecules of both hands, that is, with L- or D-configuration. For simplicity, all illustrations of individual acids as well as torsion angles discussed in this paper pertain to the L-enantiomer.

3. RESULTS AND DISCUSSION

3.1. DSC Analysis. Table 2 summarizes the temperatures, enthalpies, and entropies of DL-Abu's phase transitions. The

Table 2. Transition Temperatures (T), Enthalpies (ΔH), and Entropies (ΔS) of DL-Abu

process	T (K)	ΔH (kJ/mol)	ΔS (J/molK)
cooling	210	−0.650	−3.125
	278	−0.062	−0.227
heating	233	0.67	2.85
	346	∼0.08	∼0.24

obtained DSC thermograph with further description of the experiment is available as Supporting Information.

3.2. Space Group Distribution. As part of the JANA2006 refinement, the distributions between the $P2_1/c$ (or $B2_1/c$) and $C2/c$ space groups for *C*-DL-Abu and *D*-DL-Abu were calculated. The results given in Table 1 show that well above 50% of the crystal retain the $P2_1/c$ space group of the *A* form after transition to the *C* and *D* form; calculated fractions are 0.545(4) and 0.596(2), respectively. Coles et al. reported that the transition temperature and transition behavior for DL-Nle were "extraordinary variable",[9] and crystal-to-crystal differences with respect to diffraction properties and so forth have also been observed for DL-Abu[10] and DL-Met.[5] It would thus not be surprising if the distributions between the space groups for *C*-DL-Abu and *D*-DL-Abu are also subject to variation among different specimens

3.3. Molecular Geometry. The side chain of *A*-DL-Nva is disordered over three alternative positions as shown in Figure 4 with occupancies at 295 and 220 K given in Table 3. These figures are in good agreement with previous data for trans:gauche+:gauche− by Ichikawa and Iitaka (0.400:0.364:0.299, see above).[10] The two structures that constitute *C*-DL-Abu appear in Figure 5. In contrast to earlier results,[13] no indication of gauche rotamers were found, and the

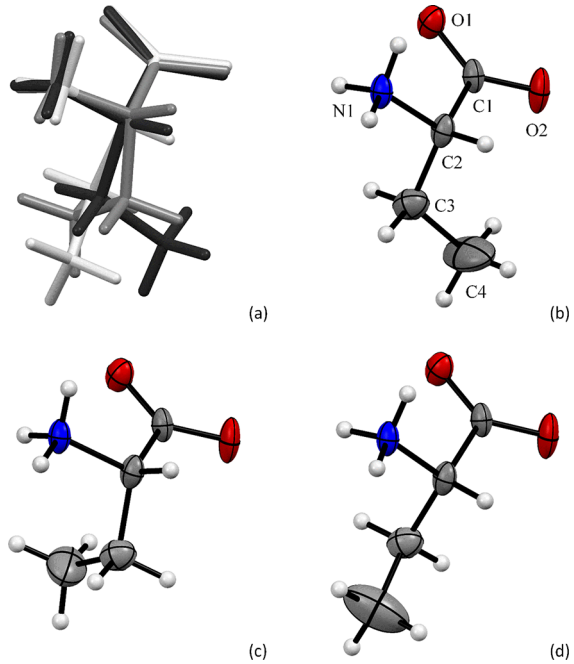

Figure 4. The molecular structure of *A*-DL-Abu at 220 K. (a) Stick drawing showing an overlay of the *trans* rotamer in black, gauche+ rotamer in gray, and gauche− rotamer in white. (b) Trans rotamer with atomic numbering. (c) Gauche+ rotamer. (d) Gauche− rotamer. In Figures 4−6, displacement ellipsoids are shown at the 50% probability level and H atoms appear as spheres of arbitrary size.

Table 3. Molecular Geometry, Occupancies for Side Chain Conformations as Defined by the N1−C2−C3−C4 Torsion Angle

molecule	temp (K)	space group	trans	gauche+	gauche−
C-DL-Nva	100	$B2_1/c$	1.000	0.000	0.000
C-DL-Nva	100	$C2/c$	1.000	0.000	0.000
A-DL-Nva	220	$P2_1/c$	0.429(2)	0.371(2)	0.200(2)
A-DL-Nva	295	$P2_1/c$	0.417(3)	0.356(2)	0.227(2)
D-DL-Nva	295	$B2_1/c$	0.332(4)	0.344(3)	0.324(5)
D-DL-Nva	295	$C2/c$	0.472(6)	0.250(4)	0.278(7)

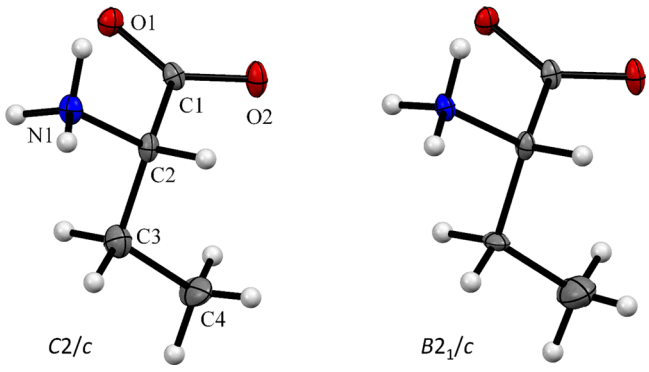

Figure 5. The molecular structure of *C*-DL-Abu at 100 K; space groups for the two parallel phases are indicated.

side chain is consequently fully ordered for both space groups and is confined to the trans orientation.

Finally, the molecular structure of *D*-DL-Abu in the space group $B2_1/c$ is shown in Figure 6 (a similar drawing of the $C2/c$ phase is available as Supporting Information). As for the *C*

dx.doi.org/10.1021/jp305016k | J. Phys. Chem. B 2012, 116, 10715−10721

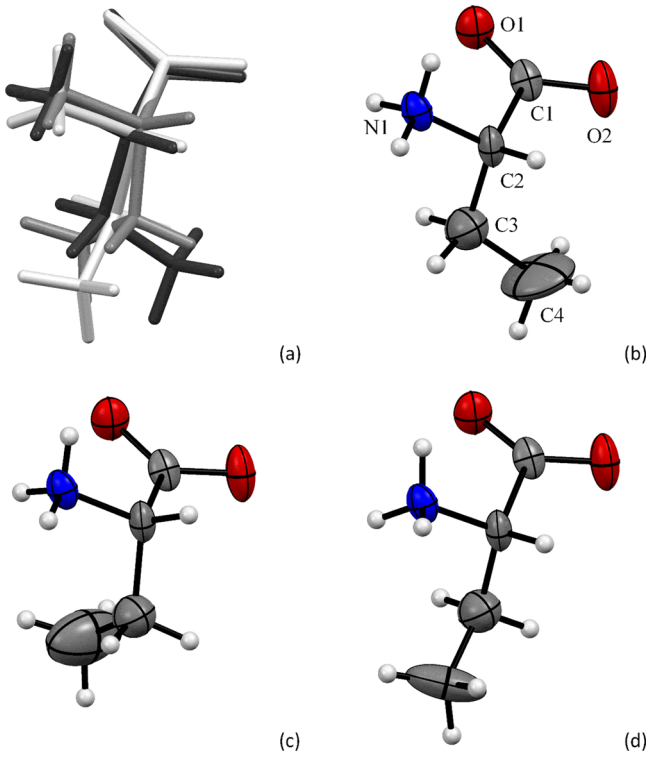

Figure 6. The molecular structure of *D*-DL-Abu at 295 K in space group $B2_1/c$. (a) Stick drawing showing an overlay of the trans rotamer in black, gauche+ rotamer in gray, and gauche− rotamer in white. (b) Trans rotamer with atomic numbering. (c) Gauche+ rotamer. (d) Gauche− rotamer.

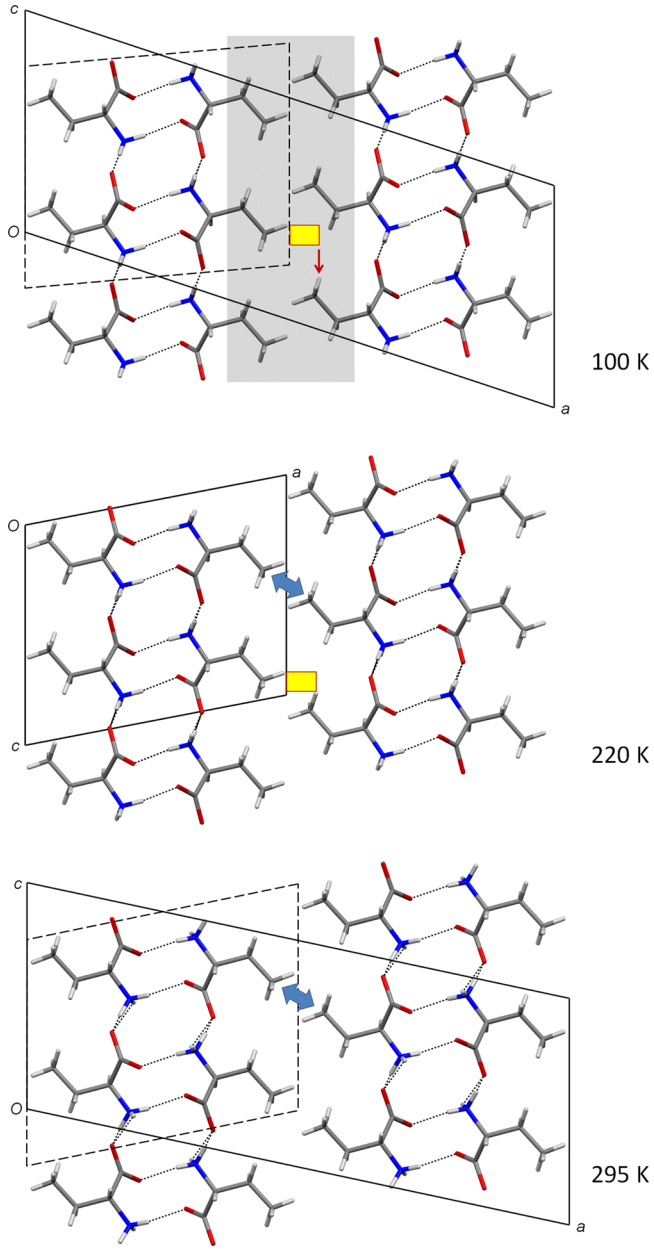

Figure 7. Crystal packing of $P2_1/c$ or $B2_1/c$ DL-Abu structures. $B2_1/c$ unit cells were used at 100 and 295 K; the alternative $P2_1/c$ unit cells are indicated by dashed lines. For the disordered structures at 220 and 295 K, only the trans orientation of the side chain has been shown. Double arrows indicate potential steric conflict, while the small, yellow rectangles highlight the translation in going from 220 to 100 K; see text for details. The gray rectangle for 100 K indicates a hydrophilic bilayer with its thickness being calculated as the separation between planes going through the centers of the C2−C3 bonds at either side.

form, all potential conformations are populated, Table 3, and not just trans and gauche− as suggested from previous work.[14] For the $P2_1/c$ phase, the distribution is almost 1:1:1 (or 0.33:0.33:0.33), while a slight preference for trans is indicated for the $C2/c$ phase.

3.4. Hydrogen Bonds. Unlike the unusual structure of the tetragonal polymorph of DL-Abu,[10,11] which packs ethyl side chains into hydrophobic columns within a three-dimensional hydrogen-bonding pattern, other DL-Abu polymorphs form structures that are divided into hydrophobic and hydrophilic layers, Figure 2. As expected for a racemate of an amino acid with an unbranched side chain, the hydrogen-bonding patterns belong to the LD−LD class[24,25] meaning that each of the two antiparallel sheets constituting a hydrogen-bonded layer in the crystal comprises amino acids of both L- and D-configuration in distinction to, for example, the two polymorphs of DL-valine[26,27] where amino acids with different chiralities are separated into independent sheets giving L1−D1 class structures.[24,25] Because of the extensive disorder, it is not meaningful to tabulate geometric parameters for these interactions for the *A* and *D* forms, but a hydrogen-bonding table for the ordered *C* form together with an illustration is provided as Supporting Information.

3.5. $P2_1/c$ ($B2_1/c$) Crystal Packing. We consider first how the $P2_1/c$ space group (refined as $B2_1/c$, see above) depends on the temperature. The illustration in Figure 7 shows that the structures of *A*-DL-Abu (220 K) and the $B2_1/c$ phase of *D*-DL-Abu (295 K) are very similar and share the same prohibitively short H···H contacts <1.8 Å if side chains are all forced into trans conformations. This conflict efficiently limits the actual occupancy of the trans rotamer to 0.500 or less, as an amino acid with a trans side chain cannot be opposing another amino acid that is also trans. As the temperature is reduced to 100 K with transition to *C*-DL-Abu, a 1.4 Å translation along the *c* axis relieves these short contacts. Accordingly, there are no intermolecular H···H contacts shorter than 2.8 Å for trans orientation of the side chains, which becomes the only observed conformation.

3.6. Molecular Volumes. The *A*- to *C*-DL-Abu transition is accompanied by an increase in the thickness of the hydrophobic layers from 5.54 to 5.64 Å, and the length of the *c*-axis also

dx.doi.org/10.1021/jp305016k | J. Phys. Chem. B 2012, 116, 10715−10721

increases from 9.8598(7) at 220 K to 9.8854(7) at 100 K. The only way the molecular volume (V_M in Table 1) manages to marginally decrease from 138.01(2) to 136.85(2) Å^3 is by reducing the length of the *b* axis from 4.8004(4) to 4.7114(4) Å. For the two *A* and *D* form structures at 295 K, the difference is even smaller, just 0.54 Å^3 per molecule or about 0.4%. These shifts are significantly smaller than those observed for other racemates in the series and may be compared with, for example, the 7.1% shift for the α- to β-transition for DL-Nva. One may speculate that these minute changes can be linked to the unusually wide hysteresis of DL-Abu, Figure 1, as changes to molecular volume appear to be an almost insignificant factor during phase transition.

3.7. Comparison between $P2_1/c$ and $C2/c$ Structures. A comparison between the two crystal phases of C-DL-Abu is given in Figure 8. They not only share the same unit cell

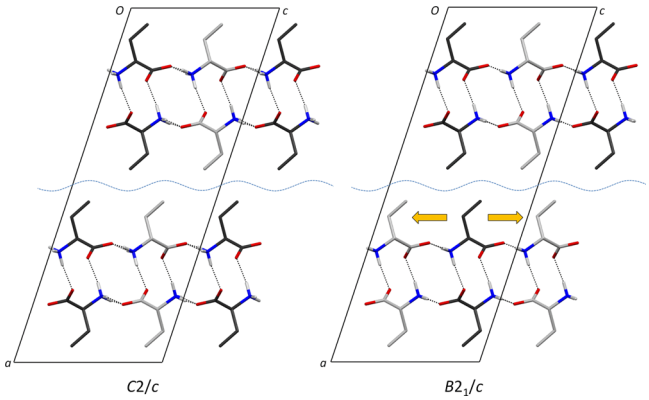

Figure 8. Crystal packing of C-DL-Abu at 100 K in the $C2/c$ and $B2_1/c$ space groups. Molecules with S-configuration (L-enantiomers) are depicted with C-atoms in light gray, and D-enantiomers are shown with dark C-atoms. The dashed curves indicate the interfaces at the centers of the hydrophobic bilayers, and arrows highlight shifts of half a unit cell length in the positive (right arrow) or negative (left arrow) direction along the *c* axis in going from the $B2_1/c$ to the $C2/c$ structure.

dimensions (by default from the refinement), but they also appear very similar indeed. The only noticeable difference is the translation half a unit cell length in either direction along the *c*-axis as indicated by the yellow arrows. There is additional translation in the viewing direction *b* as shown in Figure 2. The mixing of phases suggests that the two packing alternatives have roughly the same energy, meaning that interactions at the two hydrophobic surfaces indicated by dashed waves in Figure 8 must be very similar. Figure 9 shows that this is indeed correct; side chain ethyl groups fit into grooves in the adjacent surface in very much the same way in contrast to, for example, α- and β-DL-Nle,[3,4] where molecular conformations are also similar but with distinctly different fits at the hydrophobic interfaces (Supporting Information).

3.8. Phase Transitions. Figure 2 compared the two phase transitions of DL-Nle and showed that the $\alpha \rightarrow \gamma$ transition, in addition to the shifts along the *b*- and *c*-axes shared with the $\alpha \rightarrow \beta$ transition, also involves a conformational change for the side chain. For DL-Abu, the summary given in Table 3 indicates that the corresponding $A \rightarrow D$ transition between the intermediate and high temperature is much less profound than the $A \rightarrow C$ transition, which not only involves a slightly larger fraction of the crystal but furthermore results in ordering

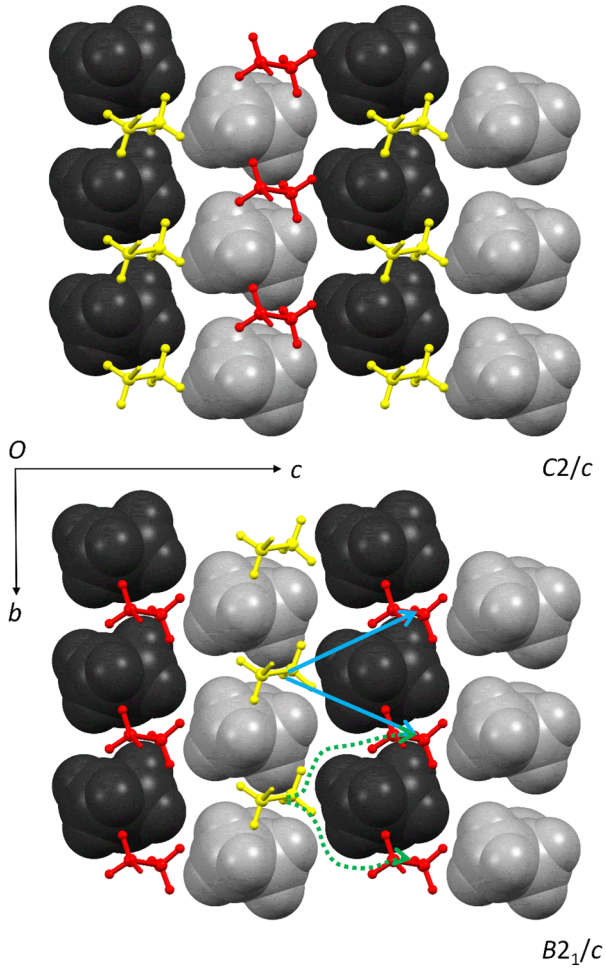

Figure 9. Fit between the hydrophobic surfaces for C-DL-Abu in the two crystal phases. One layer of side chains, corresponding to the layer above the dashed line in Figure 8, is depicted in space fill representation. L-Enantiomers are shown in yellow/light gray, while D-enantiomers are shown in red/dark gray. The blue, straight arrows show the direct shifts between space groups, and the curved, dashed lines represent suggested low-energy paths for converting one to the other.

of the side chains, which is rendered possible by a 1.4 Å shift along the *c*-axis. Accordingly, the latter transition gives a strong signal in the DSC analysis, while the signal for the $A \rightarrow D$ transition is very weak.

Table 4. Comparison between the Two Phase Transitions for DL-Abu

property \ transition	$A \rightarrow C$	$A \rightarrow D$
side chain conformation	disorder → trans	disorder → disorder
translation along a^*[a]	0.1 Å	0.2 Å
translation along c[b]	1.4 Å	~0 Å
fraction converted to $C2/c$	45.5%	40.4%

[a]Translation along a^* changes the thickness of hydrophobic bilayers as shown in Figure 7. [b]Values apply to the part of the structure that retains the $P2_1/c$ ($B2_1/c$) space group. Additional shifts for the $C2/c$ space group are 0.5 axis lengths along the *b*- and *c*-axes. There are virtually no translations along *b* for the $P2_1/c$ part.

dx.doi.org/10.1021/jp305016k | J. Phys. Chem. B 2012, 116, 10715−10721

4. CONCLUSIONS

In this study, single crystal X-ray diffraction has been used to redetermine the solid-state structures of the three monoclinic polymorphs of the amino acid racemate DL-aminobutyric acid. The new results for the ambient temperature *A* form are in agreement with previous investigations, although more detailed information has been obtained. For the low-temperature *C* form, previously thought to display equivalent side chain disorder, we have shown that the side chain is in fact ordered and limited to the trans conformation. Uniquely among the racemates of amino acids with linear side chains, the transition from the intermediate phase $P2_1/c$ to the low-temperature $C2/c$ phase is not complete meaning that below the transition temperature the crystal exists as a mixture of two space groups. Similarly, a mixture of two monoclinic phases, both with side chain disorder, is observed above the transition temperature to the *D* form. The reasons why two space groups may be simultaneously present for this particular racemate are probably related to the insignificant changes to molecular volumes upon phase transitions as well as to the almost indistinguishable hydrophobic interfaces at the center of the hydrophobic layers for the alternative molecular arrangements. The observations made here account for some unexplained features of the diffraction patterns of DL-Abu in the past and may also be relevant for the phase transitions of other related amino acids.

■ ASSOCIATED CONTENT

Ⓢ Supporting Information

Data and diagrams for the DSC analysis of DL-Abu. Hydrogen bonding data. Additional illustrations of molecular geometry. This material is available free of charge via the Internet at http://pubs.acs.org.

■ AUTHOR INFORMATION

Corresponding Author

*E-mail: c.h.gorbitz@kjemi.uio.no. Tel: +47 2285 5460. Fax: +47 2285 5441.

Notes

The authors declare no competing financial interest.

■ ACKNOWLEDGMENTS

The authors are grateful to Professor Pavel Karen, University of Oslo, for help with the DSC experiments.

■ REFERENCES

(1) Dawson, B; Mathieson, A. McL. *Acta Crystallogr.* **1951**, *4*, 475−477.
(2) Görbitz, C. H. *J. Phys. Chem. B* **2011**, *115*, 2447−2453.
(3) Harding, M. L.; Kariuki, B. M.; Williams, L. *Acta Crystallogr.* **1995**, *B51*, 1059−1062.
(4) Dalhus, B.; Görbitz, C. H. *Acta Crystallogr.* **1996**, *C52*, 1761−1764.
(5) Taniguchi, T.; Takaki, Y.; Sakurai, K. *Bull. Chem. Soc. Jpn.* **1980**, *53*, 803−804.
(6) Alagar, M.; Krishnakumar, R. V.; Mostad, A.; Natarajan, S. *Acta Crystallogr.* **2005**, *E61*, o1165−o1167.
(7) Mnyukh, Y. V.; Panfilova, N. A.; Petropavlov, N. N.; Uchvatova, N. S. *J. Phys. Chem. Solids* **1975**, *36*, 127−144.
(8) Anwar, J.; Tuble, S. C.; Kendrick, J. *J. Am. Chem. Soc.* **2007**, *129*, 2542−2547.
(9) Coles, S. J.; Gelbrich, T.; Griesser, U. J.; Hursthouse, M. B.; Pitak, M.; Threlfall, T. *Cryst. Growth Des.* **2009**, 4610−4612.
(10) Ichikawa, T.; Iitaka, Y. *Acta Crystallogr.* **1968**, *B24*, 1488−1501.
(11) Voogd, J.; Hulscher, J. B. *Acta Crystallogr.* **1980**, *B36*, 3178−3179.
(12) Voogd, J.; Derissen, J. L. *Acta Crystallogr.* **1980**, *B36*, 3175−3177.
(13) Akimoto, T.; Iitaka, Y. *Acta Crystallogr.* **1972**, *B28*, 3106−3107.
(14) Nakata, K.; Takaki, Y.; Sakurai, K. *Acta Crystallogr.* **1980**, *B36*, 504−506.
(15) Chatzigeorgiou, P; Papakonstantopoulos, N.; Tagaroulia, N.; Pollatos, E.; Xynogalas, P; Viras, K. *J. Phys. Chem. B* **2010**, *114*, 1294−1300.
(16) Bevis, M. J.; Allan, P. S. *Surf. Def. Prop. Solids* **1974**, *3*, 93−131.
(17) Ren, P.; Reichert, D.; He, Q.; Zhang, L.; Tang, H. *J. Phys. Chem. B* **2011**, *115*, 2814−2823.
(18) Allen, F. H. *Acta Crystallogr.* **2002**, *B58*, 380−388.
(19) *APEX2*; Bruker AXS Inc.: Madison, WI, USA, 2007.
(20) *SAINT-Plus*; Bruker AXS Inc.: Madison, WI, USA, 2007.
(21) *SADABS*; Bruker AXS Inc.: Madison, WI, USA, 2007.
(22) Sheldrick, G. M. *Acta Crystallogr.* **2008**, *A64*, 112−122.
(23) Petrícek,V.; Dusek, M.; Palatinus, L. *Jana2006. The crystallographic computing system*; Institute of Physics: Praha, Czech Republic, 2006.
(24) Görbitz, C. H.; Vestli, K.; Orlando, R. *Acta Crystallogr.* **2009**, *B65*, 393−400.
(25) Görbitz, C. H.; Rissanen, K.; Valkonen, A.; Husabø, Å. *Acta Crystallogr.* **2009**, *C65*, o267−o272.
(26) Flaig, R.; Koritsansky, T.; Dittrich, B.; Wagner, A.; Luger, P. *J. Am. Chem. Soc.* **2002**, *124*, 3407−3417.
(27) Mallikarjunan, M.; Rao, S. T. *Acta Crystallogr.* **1969**, *B25*, 296−303.